Intramolecular isotope effects during permanganate oxidation and acid hydrolysis of methyl tert-butyl ether

Maxime Julien, Didier Gori, Patrick Höhener, Richard Robins, Gerald Remaud

Intramolecular isotope effects during permanganate oxidation and acid hydrolysis of methyl *tert*-butyl ether

Maxime Julien*[1,3], Didier Gori[2], Patrick Höhener[2], Richard J. Robins[3], Gérald S. Remaud[3]

[1] Department of Environmental Chemistry and Engineering, Tokyo Institute of Technology, 4259 Nagatsuta-cho, Midori-ku, Yokohama, Kanagawa 226-8503, Japan.

[2] University of Aix-Marseille-CNRS, Laboratoire Chimie Environnement – UMR 7376, place Victor Hugo 3, 13331 Marseille, France.

[3] EBSI team, CEISAM, University of Nantes-CNRS UMR 6230, 2 rue de la Houssinière BP 92208, F-44322 Nantes, France.

Correspondence: M. Julien; e-mail: julien.m.aa@m.titech.ac.jp

Abstract

Stable isotopes have been widely used to monitor remediation of environmental contaminants over the last decades. This approach gives a good mechanistic description of natural or assisted degradation of organic pollutants, such as methyl *tert*-butyl ether (MTBE). Since abiotic degradation seems to be the most promising assisted attenuation method, the isotopic fractionation associated with oxidation and hydrolysis processes need to be further investigated in order to understand better these processes and make their monitoring more efficient. In this study, position-specific isotope effects (PSIEs) associated with permanganate oxidation and acid hydrolysis of MTBE were determined using isotope ratio monitoring by ^{13}C Nuclear Magnetic Resonance (irm-^{13}C NMR) combined with isotope ratio monitoring Mass Spectrometry (irm-MS). The use of this Position-Specific Isotopic Analysis (PSIA) method makes it possible to observe a specific normal IE associated with each of these two abiotic degradation mechanisms. The present work demonstrates that the ^{13}C isotope pattern of the main degradation product, *tert*-butyl alcohol (TBA), depends on the chemical reaction by which it is produced. Furthermore, this study also demonstrates that PSIA at natural abundance can give new insights into reaction mechanisms and that this methodology is very promising for the future of modeling the remediation of organic contaminants.

Keywords

Position-specific isotope effects – isotope enrichment factor – modeling – methyl *tert*-butyl ether (MTBE) – abiotic degradation – remediation

1. Introduction

Monitoring *in situ* degradation and bioremediation of groundwater pollutants is a major environmental challenge in which Compound Specific Isotope Analysis (CSIA) is today a routine technique (Hofstetter and Berg 2011). Measuring the isotopic signature of a molecule gives information pertinent to determining its origin and fate, as already demonstrated in many areas of research: geochemistry, forensics, pharmacology and environmental sciences (Aelion et al. 2010). In most cases, CSIA is performed using isotope ratio monitoring by Mass Spectrometry (irm-MS) targeting mostly ^{13}C and ^{2}H in organic contaminants (Elsner et al. 2012; Thullner et al. 2012). This analytical technique can be used routinely to determine isotopic compositions of a large range of compounds with a high precision (SD for $^{13}C \simeq 0.3‰$) and requires only a small amount of product (about 1 mg depending on the chemical composition and the analyzed element). Irm-MS can also be applied to complex mixtures when coupled to Gas Chromatography (irm-GC-MS) or High Performance Liquid Chromatography (irm-LC-MS), an interfacing that also has the advantage that sub-mg quantities can be analyzed (Meier-Augenstein 1999; Godin and McCullagh 2011).

The inconvenience of irm-MS is that it only allows a bulk ^{13}C isotope composition ($\delta^{13}C_{bulk}$ in the case of carbon) to be measured, thus averaging all carbon positions of the molecule. Hence, valuable information about the ^{13}C isotopic fractionation within molecules with numerous carbon atoms is diluted or lost completely (Bouchard et al. 2008). Knowing only the average ^{13}C isotopic composition value can be misleading when interpreting isotope effects (IEs); if $\varepsilon_{bulk} \approx 0$, does this mean that there is no fractionation or, rather, that there is a counteractive contribution of normal and inverse intramolecular

66 IEs at different positions? This conundrum can be resolved by Position-Specific Isotope
67 Analysis (PSIA), which makes possible the discrimination of those isotopomers
68 preferentially involved in a process when bulk isotope analysis only allows discriminating
69 isotopologues (Coplen 2011). Measuring position-specific isotopic composition by ^{13}C
70 Nuclear Magnetic Resonance (irm-^{13}C NMR) is now a well-established technique
71 (Jézéquel et al. 2017) employed over the last ten years to study plant metabolism (Gilbert
72 et al. 2011, 2012), pharmaceutical origin (Silvestre et al. 2009) and, more recently,
73 environmental contaminant remediation (Julien et al. 2015b, 2015a).

74 Methyl *tert*-butyl ether (MTBE) is a fuel oxygenate used as octane enhancer since the
75 1970s to replace tetraethyl lead which is a Persistent organic pollutant (POP), toxic for
76 living organisms. Despite its numerous advantages compared with lead derivatives,
77 MTBE is soluble in water, meaning that it can travel faster and farther through soil and
78 groundwater than other gasoline components (Johnson et al. 2000). For this reason it is
79 one of the most encountered pollutants met in groundwater and, even if natural
80 attenuation can be a solution, the corresponding accumulation of the metabolite *tert*-butyl
81 alcohol (TBA) could be a more problematic pollution (see Figure 1 for the chemical
82 structures of these compounds) (Kuder et al. 2005).

83 According to the literature, only a few position-specific isotopic fractionation studies
84 have been performed on organic soil pollutants. Gauchotte *et al*. studied MTBE using
85 Pyrolysis coupled with irm-MS (Py-GC-C-irm-MS) generating methanol and isobutene,
86 thus losing a part of intramolecular information on the isobutene moiety (Gauchotte et al.
87 2009). Some other partial intramolecular ^{13}C isotopic composition determinations of soil
88 pollutants have been performed using a chemical or enzymatic degradation before irm-

89 MS analysis (Huang et al. 1999). Pollutant removal has also been studied using isotopic
90 ^{2}H NMR, but working on hydrogen or oxygen, which are exchangeable, is very different
91 from observing ^{13}C distribution which observes the skeleton of the organic analyte. Irm-
92 ^{13}C NMR appears to be the only method currently able to directly determine the total
93 intramolecular isotopic composition of Volatile Organic Compounds (VOCs) such as
94 MTBE. In its initial development, it requires a larger amount of compound (around 200
95 mg) but unlike (bio)chemical degradation and Py-GC-C-irm-MS, NMR it is not a
96 destructive method so samples can be recovered.

97 MTBE is naturally removed from contaminated soil and groundwater through oxidation
98 and acid hydrolysis reaction occurring in both soil and water. Different phenomena are
99 involved in MTBE remediation and they all induce ^{13}C and/or ^{2}H isotopic fractionation.
100 Kuder *et al*. demonstrated that ^{13}C and ^{2}H isotopic fractionation are induced by passive
101 evaporation, with an inverse ^{13}C IE appearing during the process (Kuder et al. 2009).
102 Moreover, volatilization of VOCs has been proven to be associated with ^{13}C position-
103 specific isotopic fractionation (Julien et al. 2015b, 2015a). Isotopic fractionation in both ^{2}H
104 and ^{13}C have also been detected during MTBE biodegradation (Gray et al. 2002).
105 However, as natural MTBE degradation is not effective enough for a fast total remediation,
106 different technologies have been developed for the removal of MTBE (Levchuk et al.
107 2014), such as air stripping (Sutherland et al. 2004), adsorption (Hung and Lin 2006),
108 assisted biodegradation (Steffan et al. 1997) or electrochemical oxidation (Wu 2011).
109 Advanced Oxidation Processes (AOPs) seem to be the most promising method to obtain
110 a total mineralization of MTBE even if they can generate by-products which are
111 themselves potentially toxic. Many studies have been done using Fenton reagent

112 (Burbano et al. 2005, 2008), persulfate (Huang et al. 2002; Huling et al. 2011) or acid
113 hydrolysis (Elsner et al. 2007; Rosell et al. 2012) but oxidation of MTBE using
114 permanganate seems to be the most promising *in situ* method to eliminate this
115 contaminant from groundwater.

116 Oxidation of MTBE using potassium permanganate has been proven as a means to
117 rapidly clean up groundwater (Damm et al. 2002). As with other processes, MTBE
118 oxidation induces significant bulk normal ^{13}C and ^{2}H IEs (Elsner et al. 2007). The bulk
119 isotopic fractionation ($\Delta\delta^{13}C_{bulk}$) obtained during this reaction is similar to fractionation
120 observed with bioremediation with some aerobic bacterial strains such as *Methylibium*
121 *petroleiphylum* PM1 (Rosell et al. 2012). In this context, as the bulk isotope analysis does
122 not allow the (bio)degradation reaction(s) involved in the remediation to be identified, PSIA
123 using irm-^{13}C NMR could be a valuable tool to determine which process(es) are involved
124 by interpreting the measured changes in ^{13}C distribution between the carbon positions.
125 Furthermore, PSIA should be helpful in estimating the degree of MTBE remediation
126 occurring by chemical oxidation in contaminated sites, since the position-specific isotopic
127 fractionation is related directly to the mechanism of the process involved.

128 In this study, permanganate oxidation and acid hydrolysis of MTBE have been
129 performed and the resulting TBA has been purified and the ^{13}C distribution analyzed using
130 irm-MS and irm-^{13}C NMR. This data has been used to calculate position-specific
131 enrichment factors (ε_i) so as to obtain more precise information on the mechanism of these
132 processes. Determined IEs associated with both acid hydrolysis and permanganate
133 oxidation were then used to design models to observe the evolution of ^{13}C intramolecular

isotopic composition of MTBE and generated products and their concentration during these two abiotic degradation processes (see attached Excel worksheets).

2. Materials and Methods

2.1. Chemicals

Methyl *tert*-butyl ether (99.8%), potassium permanganate (≥99.8%) and sulfuric acid (96%) were obtained from Sigma-Aldrich, sodium thiosulfate (≥97%) and tris(2,4-pentadionato)chromium(III) [$Cr(Acac)_3$] were purchased from Merck, and DMSO-d_6 and acetonitrile-d_3 from Eurisotop.

2.2. Degradation experiments

Both abiotic degradations were performed in a 1 L round bottom flask. MTBE was oxidized in 600 mL of an aqueous solution of 100 mM potassium permanganate or hydrolysis was carried out using 500 mL of 250 mM aqueous sulfuric acid. The round bottom flask was closed with a turn-over flange stopper (in order to avoid MTBE evaporation) and 20 mL of pure MTBE were injected. Reactions were performed at room temperature (20-25°C) under stirring. Then, reactions were stopped by adding one equivalent (of the initial oxidant or acid) of sodium thiosulfate (100 mL at 0.6 M) or sodium hydroxide (100 mL at 1.25 M) to the oxidation or hydrolysis mixture, respectively. Afterwards, mixtures were distilled using a spinning band distillation column to purify the TBA generated by degradation, the remaining MTBE (and the generated methanol in the case of hydrolysis). A small amount (50 µL) of the distillate was employed to determine the reaction yield using ^{1}H NMR; reaction yields of 13.8% and 29.8% were measured for permanganate oxidation and acid hydrolysis, respectively. Then, remaining MTBE (and

156 methanol) were eliminated from the distillate by nitrogen purging. Finally, TBA samples
157 (containing about 35% of water) were analyzed by irm-EA-MS and irm-^{13}C NMR.

158 To measure the bulk isotope fractionation with irm-MS in MTBE, both permanganate
159 oxidation and acid hydrolysis were also performed under supposedly equal conditions but
160 on a smaller scale than the large-volume experiments described above. Oxidation was
161 done in a 20 mL vial where 0.3 mL of MTBE was dissolved in 15 mL of water. After
162 equilibration of the mixture (under stirring), 1.33 g of $KMnO_4$ were added. Acid hydrolysis
163 was also performed in a 20 mL vial in which 0.6 mL MTBE and 0.21 mL concentrated
164 sulfuric acid were dissolved in 15 mL water (final pH = 0.48). The two reactions were
165 performed at room temperature. Headspace gas (0.1 mL) was sampled every hour after
166 heating the vials at 60° C for 7 min, in order to determine δ^{13}C of the remaining MTBE.

167 2.3. Isotope ratio monitoring by Mass Spectrometry (irm-MS)

168 The bulk ^{13}C isotopic composition ($\delta^{13}C_{bulk}$) was determined by irm-MS as described
169 previously (Julien et al. 2015a). Determination of $\delta^{13}C_{bulk}$ was performed using an Integra2
170 spectrometer (Sercon Instruments, Crewe, UK) linked to a Sercon elemental analyzer
171 (EA) (Sercon Instruments, Crewe, UK) for large scale experiments. About 1 mg of each
172 sample was weighed into tin capsules (2x5 mm, Thermo Fisher scientific) using a 10^{-6} g
173 precision balance (Ohaus Discovery DV215CD) in order to ensure analysis of 0.2-0.8 mg
174 of carbon. Bulk ^{13}C isotope analysis of MTBE samples from headspace of 20 mL vial
175 reactions was performed using a Delta V advantage (Thermo Fisher Scientific) connected
176 to a Gas Chromatography (Trace 1310, Thermo Fisher Scientific) equipped with a TG-
177 5MS column (60 m x 0.25 mm i.d., 0.25 μm film thickness, Thermo Fisher Scientific) via a

178 CONFLOW-II interface. $\delta^{13}C_{bulk}$ (‰) values were expressed relative to the international
179 reference (Vienna-Pee Dee Belemnite, V-PDB) using the equation 1:

180 $$\delta^{13}C_g\ (‰) = \left(\frac{R_{sample}}{R_{standard}} - 1\right) \times 1000 \qquad (1)$$

181 For $\delta^{13}C_{bulk}$ determination, the laboratory standard of glutamic acid used for irm-EA-MS
182 and the CO_2 reference gas for irm-GC-MS analyses were calibrated against the
183 international reference material.

184 2.4. Isotope ratio monitoring by ^{13}C Nuclear Magnetic Resonance spectrometry (irm-
185 ^{13}C NMR)

186 The position-specific ^{13}C isotopic composition ($\delta^{13}C_i$, where i is the corresponding
187 carbon position) was determined as described previously (See Supporting Information for
188 more details) (Julien et al. 2015b). The TBA sample was prepared in a 4 mL vial in which
189 100 µL of the lock substance (DMSO-d_6) containing 50 mM of the relaxing agent $Cr(Acac)_3$
190 were introduced. DMSO-d_6 was chosen because of its miscibility with TBA and water and
191 to avoid peak overlapping on the ^{13}C spectrum between the sample and the deuterated
192 solvent. The amount of $Cr(Acac)_3$ was adapted according to the T_1 values (longitudinal
193 relaxation). Then, 600 µL of sample are added and, after mixing, the sample was
194 introduced into a 5 mm NMR tube. MTBE NMR measurements were performed in the
195 same way but with the following sample preparation: 500 µL of MTBE mixed with 200 µL
196 of acetonitrile-d_3 containing 200 mM of $Cr(Acac)_3$.

197 ^{13}C NMR spectra of both MTBE and TBA were recorded using a Bruker AVANCE I 400
198 MHz spectrometer fitted with a 5 mm i.d. $^{1}H/^{13}C$ dual^{+} probe, carefully tuned at the

199 recording frequency of 100.61 MHz. Detailed explanation of the isotopic ^{13}C NMR protocol
200 and $\delta^{13}C_i$ calculation is available in Supporting Information.

201 2.5. Determination of enrichment factors (ε)

202 For large scale degradation experiments, ^{13}C Isotope Effects associated with both
203 permanganate oxidation and acid hydrolysis were calculated using the t_0 value and a
204 single data point. This method of calculating the enrichment factor has already been
205 shown to provide very similar results to the classical Rayleigh plot method which requires
206 multiple data points (Jeannottat and Hunkeler 2012). Moreover, a recently published study
207 has demonstrated that this "two point calculation" (t_0 and one experimental point) gives
208 the same result as a Rayleigh plot when less than 30% of MTBE has reacted (Julien et al.
209 2018). In order to quantify bulk and position-specific enrichment factors, the equation 2,
210 adapted from that work, has been used in the present work:

211 $$\varepsilon = \frac{\delta^{13}C_{MTBE} - \delta^{13}C_{TBA}}{\left(\frac{f}{1-f}\right) \times \ln} \qquad (2)$$

212 where *f* is the reaction yield, $\delta^{13}C_{MTBE}$ is the bulk ($\delta^{13}C_{Bulk}$) or position-specific ($\delta^{13}C_i$)
213 isotopic composition of MTBE used as reactant in abiotic degradation experiments and
214 $\delta^{13}C_{TBA}$ is the bulk ($\delta^{13}C_{Bulk}$) or position-specific ($\delta^{13}C_i$) isotopic composition of TBA. When
215 ε_i (position-specific enrichment factor) is calculated, the $\delta^{13}C_i$ of the corresponding carbon
216 position is used for both MTBE and TBA. In this calculation, the bulk $\delta^{13}C_{MTBE}$ cannot be
217 used directly in the calculation but the average value of the quaternary carbon and the
218 methyl groups of MTBE (corresponding to the carbon atoms of the reaction product, TBA
219 see Figure 1) need to be used in order to calculate the bulk IE associated with the

generation of TBA from MTBE. When ε is negative, the IE is considered as normal (light isotopologues are preferentially used during the process) and when ε is positive, the IE is inverse (transformation is faster for heavy isotopologues).

In the case of smaller scale experiments, $\delta^{13}C$ of MTBE was monitored using irm-GC-IRMS. In this context, Rayleigh plots ($1000*\ln(\delta+1000)/(\delta_0+1000)$) vs $\ln(f)$) were drawn and ε corresponds to the slope of the regression curve (see Figure S3 in the Supporting Information).

Finally, in order to determine the significance threshold of the measured enrichment factors, the expanded uncertainty (U) has been calculated. The calculation of U associated with ε takes into account all sources of uncertainty generated by weighing of compounds or the measurement of the reaction yield. While most studies only use the standard deviation (SD) of the isotopic measurement, U gives a better assessment of accuracy. The calculation of U has been fully described in a previous study (Julien et al. 2018) and results are expressed as $\varepsilon \pm U$ in this article (note that results from cited articles are expressed as ε or $\Delta\delta^{13}C \pm 1SD$).

2.6. Position-specific modeling of isotope ratiosA model for the temporal evolution of the isotope ratio at each specific position during the reaction of MTBE was developed based on equations which were published previously (Höhener et al, 2017). The model was modified in the sense that no transport in a groundwater system is included, but it was extended in order to include the isotope evolution of the formed products as well. The model is an Excel spreadsheet and is provided in Appendix A. A detailed description of all model equations is included in this spreadsheet.

3. Results and discussion

3.1. Reaction rates and bulk isotope analysis

The change in concentration of MTBE for both abiotic transformation reactions followed a first-order type kinetics, with half-life times of 0.33 and 5.7 per day for permanganate oxidation and hydrolysis, respectively. These rates are similar to previously published rates (Elsner et al., 2007; Gauchotte et al., 2009). The monitoring of the bulk MTBE ^{13}C isotope enrichment allowed ε values of -4.9 ± 0.2‰ and -6.4 ± 0.6‰ (see Table 1) to be obtained for permanganate oxidation and acid hydrolysis, respectively, which is also in accordance with previous data found in the literature. In previous studies, Rosell et al. 2012 described ε values of -5.5 ± 0.1‰ and -6.1 ± 0.1‰ for permanganate oxidation and acid hydrolysis respectively, Elsner et al. 2007 measured ε of -4.9 ± 0.2‰ associated with acid hydrolysis and Gauchotte et al. 2010 determined ε of -4.9 ± 0.6‰ in the case of permanganate oxidation (see Table 1).

In the present study, the bulk isotope effect was also monitored using the product of the reaction, TBA. The present study shows that large scale permanganate oxidation and acid hydrolysis are both associated with a normal bulk ^{13}C IE according to their ε values of -1.9 ± 0.7‰ and -3.8 ± 0.7‰ obtained from the product TBA, respectively (see Table 1). Note that most isotope fractionation studies found in literature are performed analyzing the remaining substrate, but in this study the reaction product was also analyzed. However, it must be noted that TBA is not the only product (the methyl carbon left) and therefore it is logical that the value for the isotope effect obtained from the product does not relate directly to the value obtained from the substrate.

264 Nonetheless, the results all agree that the abiotic degradation velocity is higher with
265 light MTBE isotopologues (molecules containing ^{12}C isotope) (Bigeleisen 1949), in
266 accordance with the principles of reaction rate theory in the presence of heavy isotopes
267 (Haring 1942). Since a $^{13}C–^{12}C$ bond is shorter than a $^{12}C–^{12}C$ bond and the vibrational
268 energy of shorter bonds is smaller (lower zero point energy), the activation energy needed
269 to break a $^{13}C–^{12}C$ bond is higher than for a $^{12}C–^{12}C$ bond. In the conditions studied,
270 abiotic degradation of MTBE apparently preferentially uses light substrate, as normal IEs
271 are detected.

272 3.2. Position-specific isotope analysis – oxidation

273 In the present work, PSIA performed using isotopic ^{13}C NMR showed an unbalanced
274 distribution of normal IEs associated with MTBE oxidation by potassium permanganate.
275 Despite a relatively small $\delta^{13}C_{Bulk}$ it is found that this abiotic degradation process is
276 associated with a strong normal IE on the quaternary carbon (ε = -10.1 ± 0.7‰) and
277 negligible IEs on the methyl groups (ε = +0.8 ± 0.7‰, see Table 1). The degradation
278 mechanism of oxidation of MTBE by potassium permanganate has been described
279 previously (for a detailed description, see Figure 2) (Damm et al. 2002; Elsner et al. 2007)
280 and it is considered that it is initiated by H abstraction from the methyl of the methoxy
281 group, leading to oxidation and bond breakage via an S_N2 reaction mechanism. This
282 reaction scheme is compatible with both the observed high secondary normal IE on the
283 quaternary carbon, which is in α position to the broken bond, and the absence of
284 significant IE on the methyl groups, which are inert during the degradation mechanism.
285 This theory is confirmed by results of the present study and those from Gauchotte *et al*.
286 (2009) who determined the ^{13}C isotopic fractionation ($\Delta\delta^{13}C$) occurring during MTBE

287 oxidation using pyrolysis coupled with GC-C-irm-MS. This method allowed the
288 observation of the isotopic composition of the methoxy group and an average value of the
289 central carbon and methyl positions of MTBE. These experiments showed a large ^{13}C
290 enrichment in the methoxy group and no significant change in ^{13}C isotopic composition of
291 other carbon positions of the remaining MTBE. Results from these studies demonstrate
292 that the bond breaking (between the oxygen atom and the methoxy group) occurring
293 during permanganate oxidation of MTBE is associated with a primary normal ^{13}C IE on
294 the methoxy group and a strong secondary normal ^{13}C IE on the quaternary carbon
295 position.

296 3.3. Position-specific isotope analysis – hydrolysis

297 In the case of acid hydrolysis, irm-^{13}C NMR analysis indicates a very different
298 distribution of the $\delta^{13}C_i$ values contributing to the observed $\delta^{13}C_{Bulk}$ normal IE to that of
299 permanganate oxidation. Acid hydrolysis catalyzed by sulfuric acid is associated with a
300 normal IE distributed between the quaternary carbon (ε = -3.2 ± 0.7‰) and the methyl
301 groups (ε = -4.0 ± 0.7‰), see Table 1. Measuring different PSIEs is not surprising, given
302 that the mechanism of reaction is considered to be very different from that of
303 permanganate oxidation (see Figure 2). In the hydrolysis reaction, the bond between the
304 oxygen atom and the quaternary carbon is broken, which fits with the observed large
305 primary ^{13}C IE located at this carbon position. Elsner *et al*. (2007) demonstrated that acid
306 hydrolysis is associated with a large normal IE and calculated an ε value for the central
307 carbon position (ε = -24.3 ± 2.3‰), assuming that all other carbons do not enrich (Table
308 1) (Elsner et al. 2007). The most surprising result here is the presence of secondary
309 normal IEs located on the methyl groups, however, because this part of the MTBE

310 structure is supposed not to be involved in the initial bond breaking reaction. Our results
311 show that the effect on the reactive position is smaller, as assumed by Elsner and co-
312 workers. However, acid hydrolysis is an S_N1 reaction, with a carbocation intermediate (see
313 Figure 2) and the normal IE located on the methyl groups can be proposed as due to the
314 stabilization process of this intermediate state. As a consequence, the presence of a ^{13}C
315 isotope on methyl groups could affect the stability of the carbocation intermediate and aid
316 these isotopomers to react faster during bond breaking between the quaternary carbon
317 and the oxygen atom.

318 As explained above (section 3.1.), $^{13}C–^{12}C$ bonds are more difficult to break than $^{12}C–$
319 ^{12}C, because chemical bonds involving heavy isotopes have a lower zero-point energy
320 and the activation energy required for bond breaking is greater, so heavy isotopomers are
321 more stable than light ones. According to this convention, the presence of a ^{13}C isotope
322 at the methyl positions of MTBE molecules could play a role in the stabilization of the
323 transition-state (carbocation) during the acid hydrolysis of MTBE (Figure 2). As a
324 consequence, MTBE molecules with ^{12}C on their methyl positions (light isotopomers)
325 should react faster, while heavy isotopomers form more stable carbocation intermediates.
326 This carbocation stability difference can explain the detection of a normal secondary
327 isotope effect on these carbon positions. This precept has already been described in the
328 case of enzyme catalytic activity in which the presence of heavy isotopes influences the
329 stability of the transition-state and is directly responsible for the IEs associated with
330 enzyme activity (Schramm 1998).

331 3.4. Modeling MTBE abiotic degradation

Bulk carbon isotopes are employed for (i) detecting the origin of organic contaminants, (ii) monitoring their natural or assisted remediation until their complete mineralization and (iii) understanding the mechanisms involved. The use of PSIA has already proved to be an efficient tool to determine the origin of organic contaminants such as VOCs (Julien et al. 2016) or pharmaceuticals (Silvestre et al. 2009). This method offers more parameters to identify the origin of detected pollutants compared with bulk isotope analysis, which only allows one $\delta^{13}C$ value to be determined. Moreover, PSIA has also proved its capability to detect unexpected intramolecular IEs associated with VOCs evaporation (Julien et al. 2015b, 2015a) and, more generally, effects caused by the presence of non-covalent interactions (Botosoa et al. 2008; Julien et al. 2017).

In the present study, PSIEs associated with two abiotic degradation reactions (oxidation and acid hydrolysis) of MTBE were measured. These new data strengthen our fundamental understanding of these processes by validating the two different mechanisms previously proposed in the literature (Elsner et al. 2007). A highlight of this study is the construction of a model capable of predicting isotope ratios of MTBE carbon positions as a function of time during abiotic degradation (here, acid hydrolysis or oxidation). This new model requires the measurement of the initial ^{13}C distribution in MTBE and the PSIEs measured in this article (see blue boxes in Appendix A). The initial MTBE concentration, the degradation half time and the duration of reaction can be adjusted in the Excel worksheet. Figure 3 presents the evolution of $\delta^{13}C$ on both degraded MTBE and formed TBA carbon positions. The development of this model can help predicting the isotope changes in MTBE along a contaminant plume of gasoline in

354 groundwater or soil using the 3-dimensional transport code BIOSCREEN-AT-ISO
355 (Höhener et al. 2017).

356 **4. Conclusions**

357 PSIA performed using irm-^{13}C NMR is still considered as difficult to apply for field
358 investigations because of the amount of sample needed for each analysis. However, it
359 has recently been shown that PSIA by NMR can be performed with less than 50 mg, and
360 analysis of samples of the order of 10 mg is in advanced development (Joubert et al.
361 2018). Hence, PSIA by ^{13}C NMR targeting TBA could be an excellent tool for mechanism
362 elucidation and modeling of natural processes, such as environmental contaminant
363 remediation. PSIA is shown to give a more detailed picture of the isotopic fractionation
364 during abiotic remediation processes, distinguishing which isotopomers are preferentially
365 involved in the reaction system. The determination of position-specific isotopic
366 composition provides a more detailed dataset, crucially, one that indicates which
367 mechanism of reaction was involved in the degradation. Thus, it can act as a useful
368 indicator of which remediation processes may be dominant during the remediation of an
369 organic pollutant, such as MTBE. As already explained, permanganate oxidation and acid
370 hydrolysis of MTBE are both associated with a similar normal bulk IE, which does not give
371 access to detail of the observed abiotic degradation process. In contrast, PSIA shows a
372 large variation of the IE distribution between the two studied reactions, which means that
373 the different processes involved in remediation can be distinguished by using the
374 measured intramolecular ^{13}C isotope signatures, thus offering a new tool to monitor
375 contaminant removal. Intramolecular IEs measured *in vitro* using irm-^{13}C NMR combined
376 with designed models predicting the evolution of ^{13}C distribution in MTBE and its

377 degradation products (see attached Excel worksheet) is a new efficient tool for monitoring
378 soil contamination by gasoline-derived pollutants.

379 Complementary investigations are now required to underpin the interpretation of these
380 observed position-specific IEs in terms of the proposed reactions mechanisms. The
381 determination of ^{18}O IEs would be of interest, as these should differ considerably between
382 the permanganate oxidation and acid hydrolysis, because the oxygen atom of TBA comes
383 from MTBE in the case of oxidation while it is added from water during acid hydrolysis
384 (Figure 2). This, however, requires purifying the TBA from water without introducing
385 isotopic fractionation. Theoretical calculations should also help to relate the observed IEs
386 to mechanism (Wolfsberg et al. 2009), but these have proved challenging and are beyond
387 the scope of the present report. It is evident that PSIA gives new clues about
388 environmental contaminant removal and can be used for modeling, as already shown in
389 the case of tetrachloroethene (Höhener and Atteia 2014). The constant improvement in
390 terms of sensitivity, precision and complexity of analyzed structures of PSIA techniques,
391 including more sensitive irm-^{13}C NMR (Jézéquel et al. 2017), Py-GC-C-irm-MS (Gilbert et
392 al. 2016) and the recent proof of concept for high resolution MS (Eiler et al. 2017) assure
393 that PSIA can be an excellent tool for the future of monitoring of organic contaminant
394 remediation.

395

396 **Appendix A. Model of permanganate oxidation and acid hydrolysis of MTBE**

397 **Appendix B. Supplementary material**

398

Acknowledgements

This work is funded by the French National Research Agency ANR, project ISOTO-POL funded by the program CESA (no. 009 01). M.J. thanks the ANR for funding his PhD bursary through this project and JSPS for funding his postdoctoral fellowship. We thank Dr. Martin Elsner for his help in understanding reaction mechanisms.

References

Aelion MC, Höhener P, Hunkeler D, Aravena R. Environmental Isotopes in Biodegradation and Bioremediation. Taylor & Francis Group; 2010.

Bigeleisen J. The Relative Reaction Velocities of Isotopic Molecules. J Chem Phys. 1949;17(8):675–8.

Botosoa EP, Caytan E, Silvestre V, Robins RJ, Akoka S, Remaud GS. Unexpected fractionation in site-specific 13C isotopic distribution detected by quantitative 13C NMR at natural abundance. J Am Chem Soc. 2008 Jan 1;130(2):414–5.

Bouchard D, Hunkeler D, Höhener P. Carbon isotope fractionation during aerobic biodegradation of n-alkanes and aromatic compounds in unsaturated sand. Org Geochem. 2008 Jan 1;39(1):23–33.

Burbano AA, Dionysiou DD, Suidan MT. Effect of oxidant-to-substrate ratios on the degradation of MTBE with Fenton reagent. Water Res. 2008;42(12):3225–39.

Burbano AA, Dionysiou DD, Suidan MT, Richardson TL. Oxidation kinetics and effect of pH on the degradation of MTBE with Fenton reagent. Water Res. 2005;39(1):107–18.

Coplen TB. Guidelines and recommended terms for expression of stable-isotope-ratio and gas-ratio measurement results. Rapid Commun Mass Spectrom. 2011;25(17):2538–60.

Damm JH, Hardacre C, Kalin RM, Walsh KP. Kinetics of the oxidation of methyl tert-butyl ether (MTBE) by potassium permanganate. Water Res. 2002;36(14):3638–46.

Eiler J, Cesar J, Chimiak L, Dallas B, Grice K, Griep-Raming J, et al. Analysis of molecular isotopic structures at high precision and accuracy by Orbitrap mass spectrometry. Int J Mass Spectrom. 2017 Nov 1;422:126–42.

Elsner M, Jochmann MA, Hofstetter TB, Hunkeler D, Bernstein A, Schmidt TC, et al. Current challenges in compound-specific stable isotope analysis of environmental organic contaminants. Anal Bioanal Chem. 2012 Jul;403(9):2471–91.

Elsner M, McKelvie J, Lacrampe Couloume G, Sherwood Lollar B. Insight into Methyl tert-Butyl Ether (MTBE) Stable Isotope Fractionation from Abiotic Reference Experiments. Environ Sci Technol. 2007 Aug 1;41(16):5693–700.

Gauchotte C, Connal G, O'Sullivan G, Kalin RM. Position Specific Isotope Analysis: The Ultimate Tool in Environmental Forensics? In: Morrison RD, O'Sullivan G, editors. Environmental Forensics: Proceedings of the 2009 INEF Annual Conference [Internet]. The Royal Society of Chemistry; 2010. p. 60–70. Available from: http://dx.doi.org/10.1039/9781849732062-00060 http://pubs.rsc.org/en/Content/Chapter/9781849732062-00060/978-1-84973-206-2

Gauchotte C, O'Sullivan G, Davis S, Kalin RM. Development of an advanced on-line position-specific stable carbon isotope system and application to methyl tert-butyl ether. Rapid Commun Mass Spectrom. 2009 Oct;23(19):3183–93.

Gilbert A, Robins RJ, Remaud GS, Tcherkez GG. Intramolecular 13C pattern in hexoses from autotrophic and heterotrophic C3 plant tissues. Proc Natl Acad Sci U S A. 2012 Oct 30;109(44):18204–9.

Gilbert A, Silvestre V, Robins RJ, Tcherkez G, Remaud GS. A 13C NMR spectrometric method for the determination of intramolecular δ13C values in fructose from plant sucrose samples. New Phytol. 2011;191(2):579–88.

Gilbert A, Yamada K, Suda K, Ueno Y, Yoshida N. Measurement of position-specific 13C isotopic composition of propane at the nanomole level. Geochim Cosmochim Acta. 2016;177:205–16.

Godin J-P, McCullagh JSO. Review: Current applications and challenges for liquid chromatography coupled to isotope ratio mass spectrometry (LC/IRMS). Rapid Commun Mass Spectrom. 2011;25(20):3019–28.

Gray JR, Lacrampe-Couloume G, Gandhi D, Scow KM, Wilson RD, Mackay DM, et al. Carbon and Hydrogen Isotopic Fractionation during Biodegradation of Methyl tert-Butyl Ether. Environ Sci Technol. 2002 May 1;36(9):1931–8.

Haring MM. The Theory of Rate Processes (Glasstone, Samuel; Laidler, Keith J.; Eyring, Henry). J Chem Educ. 1942 May 1;19(5):249.

Hofstetter TB, Berg M. Assessing transformation processes of organic contaminants by compound-specific stable isotope analysis. Trends Anal Chem. 2011;30(4):618–27.

Höhener P, Atteia O. Rayleigh equation for evolution of stable isotope ratios in contaminant decay chains. Geochim Cosmochim Acta. 2014;126(0):70–7.

Höhener, P. Li, Z. M.Julien, M. Nun, P. Robins, R. J. Remaud, G. S., 2017. Simulating compound-specific isotope ratios in plumes of groundwater pollutants with BIOSCREEN-AT-ISO. Groundwater, 55(2): 261-67.

Huang D-S, Wu S-H, Huang C-Y, Lin C-Y. An exploration of intramolecular carbon isotopic distributions of commercial acetone and isopropanol. Org Geochem. 1999;30(7):667–74.

Huang K-C, Couttenye RA, Hoag GE. Kinetics of heat-assisted persulfate oxidation of methyl tert-butyl ether (MTBE). Chemosphere. 2002;49(4):413–20.

Huling SG, Ko S, Park S, Kan E. Persulfate oxidation of MTBE- and chloroform-spent granular activated carbon. J Hazard Mater. 2011;192(3):1484–90.

Hung H-W, Lin T-F. Adsorption of MTBE from contaminated water by carbonaceous resins and mordenite zeolite. J Hazard Mater. 2006;135(1–3):210–7.

Jeannottat S, Hunkeler D. Chlorine and Carbon Isotopes Fractionation during Volatilization and Diffusive Transport of Trichloroethene in the Unsaturated Zone. Environ Sci Technol. 2012 Mar 20;46(6):3169–76.

Jézéquel T, Joubert V, Giraudeau P, Remaud GS, Akoka S. The new face of isotopic NMR at natural abundance. Magn Reson Chem. 2017 Feb 1;55(2):77–90.

Johnson R, Pankow J, Bender D, Price C, Zogorski J. Peer Reviewed: MTBE—To What Extent Will Past Releases Contaminate Community Water Supply Wells? Environ Sci Technol. 2000 May 1;34(9):210A-217A.

Joubert V, Silvestre V, Grand M, Loquet D, Ladroue V, Besacier F, et al. Full Spectrum Isotopic 13C NMR Using Polarization Transfer for Position-Specific Isotope Analysis. Anal Chem. 2018 Jul 17;90(14):8692–9.

Julien M, Gilbert A, Yamada K, Robins RJ, Höhener P, Yoshida N, et al. Expanded uncertainty associated with determination of isotope enrichment factors: Comparison of two point calculation and Rayleigh-plot. Talanta. 2018 Jan 1;176:367–73.

Julien M, Höhener P, Robins RJ, Parinet J, Remaud GS. Position-Specific 13C Fractionation during Liquid–Vapor Transition Correlated to the Strength of Intermolecular Interaction in the Liquid Phase. J Phys Chem B. 2017 Jun 15;121(23):5810–7.

Julien M, Nun P, Höhener P, Parinet J, Robins RJ, Remaud GS. Enhanced forensic discrimination of pollutants by position-specific isotope analysis using isotope ratio monitoring by 13C nuclear magnetic resonance spectrometry. Talanta. 2016;147:383–9.

501 Julien M, Nun P, Robins RJ, Remaud GS, Parinet J, Höhener P. Insights into Mechanistic
502 Models for Evaporation of Organic Liquids in the Environment Obtained by
503 Position-Specific Carbon Isotope Analysis. Environ Sci Technol. 2015a Nov
504 3;49(21):12782–8.

505 Julien M, Parinet J, Nun P, Bayle K, Höhener P, Robins RJ, et al. Fractionation in position-
506 specific isotope composition during vaporization of environmental pollutants
507 measured with isotope ratio monitoring by 13C nuclear magnetic resonance
508 spectrometry. Environ Pollut. 2015b;205:299–306.

509 Kuder T, Philp P, Allen J. Effects of volatilization on carbon and hydrogen isotope ratios
510 of MTBE. Environ Sci Technol. 2009 Mar 15;43(6):1763–8.

511 Kuder T, Wilson JT, Kaiser P, Kolhatkar R, Philp P, Allen J. Enrichment of Stable Carbon
512 and Hydrogen Isotopes during Anaerobic Biodegradation of MTBE: Microcosm
513 and Field Evidence. Environ Sci Technol. 2005 Jan 1;39(1):213–20.

514 Levchuk I, Bhatnagar A, Sillanpää M. Overview of technologies for removal of methyl tert-
515 butyl ether (MTBE) from water. Sci Total Environ. 2014;476–477(0):415–33.

516 Meier-Augenstein W. Applied gas chromatography coupled to isotope ratio mass
517 spectrometry. J Chromatogr A. 1999 May 21;842(1):351–71.

518 Rosell M, Gonzalez-Olmos R, Rohwerder T, Rusevova K, Georgi A, Kopinke F-D, et al.
519 Critical Evaluation of the 2D-CSIA Scheme for Distinguishing Fuel Oxygenate
520 Degradation Reaction Mechanisms. Environ Sci Technol. 2012 May 1;46(9):4757–
521 66.

522 Schramm VL. Enzymatic transition states and transition state analog design. Annu Rev
523 Biochem. 1998;67:693–720.

524 Silvestre V, Mboula VM, Jouitteau C, Akoka S, Robins RJ, Remaud GS. Isotopic 13C
525 NMR spectrometry to assess counterfeiting of active pharmaceutical ingredients:
526 Site-specific 13C content of aspirin and paracetamol. J Pharm Biomed Anal.
527 2009;50(3):336–41.

528 Steffan RJ, McClay K, Vainberg S, Condee CW, Zhang D. Biodegradation of the gasoline
529 oxygenates methyl tert-butyl ether, ethyl tert-butyl ether, and tert-amyl methyl ether
530 by propane-oxidizing bacteria. Appl Environ Microbiol. 1997;63(11):4216–22.

531 Sutherland J, Adams C, Kekobad J. Treatment of MTBE by air stripping, carbon
532 adsorption, and advanced oxidation: technical and economic comparison for five
533 groundwaters. Water Res. 2004;38(1):193–205.

534 Thullner M, Centler F, Richnow H-H, Fischer A. Quantification of organic pollutant
535 degradation in contaminated aquifers using compound specific stable isotope
536 analysis – Review of recent developments. Org Geochem. 2012;42(12):1440–60.

Wolfsberg M, Van Hook WA, Paneth P. Isotope Effects in the Chemical, Geological, and Bio Sciences. 2009.

Wu T-N. Electrochemical removal of MTBE from water using the iridium dioxide coated electrode. Sep Purif Technol. 2011;79(2):216–20.

Figures and Tables

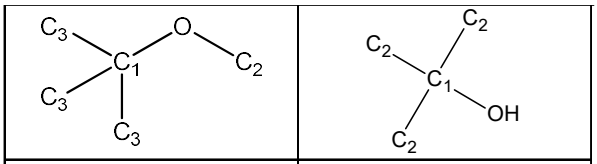

	MTBE	TBA
C_1	Quaternary carbon - C(IV)	Quaternary carbon - C(IV)
C_2	Methoxy - OCH_3	Methyl - CH_3
C_3	Methyl - CH_3	-

Figure 1: The molecular structure of Methyl *tert*-Butyl Ether and *tert*-Butanol with the carbon atoms numbered in relation to decreasing chemical shift in the ^{13}C NMR spectrum and their corresponding chemical functions.

Reaction	ε (‰) MTBE Bulk	TBA Bulk	CH_3 PSIA of TBA	C(IV) PSIA of TBA	OCH_3 calculated	reference
permanganate oxidation	-4.9 ± 0.2	-1.9 ± 0.7	+0.8 ± 0.7	-10.1 ± 0.7	-16.8 ± 1.0[a]	this study
	-4.9 ± 0.1	-	see table below ($\Delta\delta^{13}C$ values)			Gauchotte et al. 2009
	-5.5 ± 0.1	-	-	-	-	Rosell et al. 2012
acid hydrolysis	-6.4 ± 0.6	-3.8 ± 0.7	-4.0 ± 0.7	-3.2 ± 0.7	-16.8 ± 1.0[a]	this study
	-4.9 ± 0.6	-	-	-	-24.3 ± 2.3[b]	Elsner et al. 2007
	-6.1 ± 0.1	-	-	-	-	Rosell et al. 2012

Reaction	$\Delta\delta^{13}C$ (‰) MTBE	TBA	*i*-Butylene	Methanol	reference
permanganate oxidation	+6.2 ± 0.2	-	0.0 ± 0.4	+22.8 ± 0.5	Gauchotte et al. 2009

Table 1: Comparison of enrichment factors (ε) associated with permanganate oxidation and acid hydrolysis of MTBE determined in this study and values found in literature (C(IV) corresponds to the quaternary carbon of MTBE). Position-specific isotope data from Gauchotte et al. 2010[33] are expressed as isotopic fractionation ($\Delta\delta^{13}C$), so they are detailed in a separated table below.

[a]: Calculated through mass balance.

[b]: Theoretical value if no secondary isotope effects on other carbons.

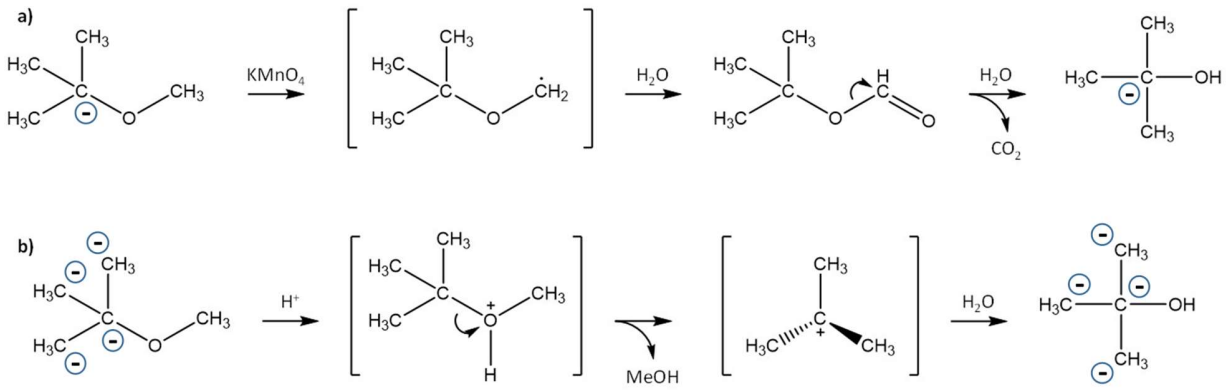

559

560 **Figure 2:** Proposed reaction mechanisms of MTBE degradation during (a) potassium
561 permanganate oxidation and (b) acid hydrolysis. The symbol "-" indicates the carbon
562 positions where a significant normal isotope effect was measured.

563

564

565

566

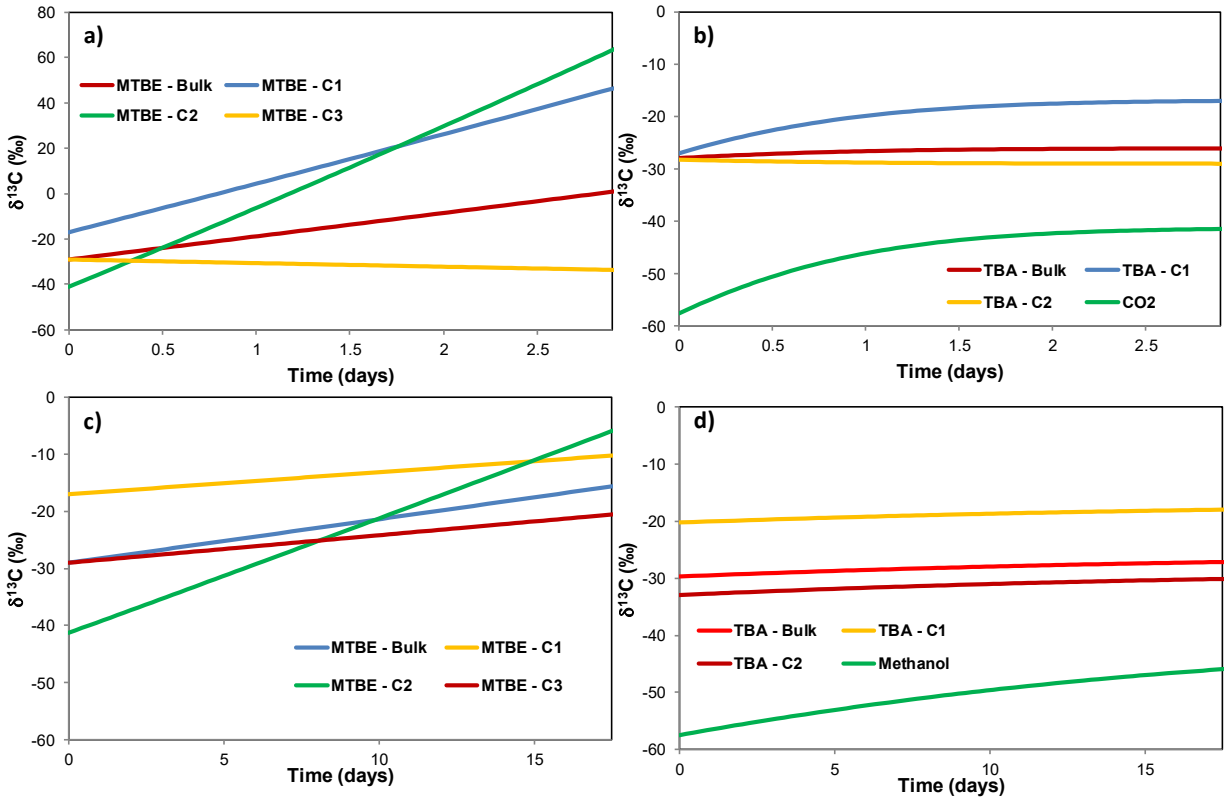

567

568 **Figure 3:** Evolution of $\delta^{13}C$ as a function of time during permanganate oxidation (a: MTBE;
569 b: reaction products) and acid hydrolysis (c: MTBE; d: reaction products). The calculations
570 were carried out using the model developed in the present study.